THERMALLY-STIMULATED DISCHARGE CURRENTS IN ICE

JoAnne L. Huppunen

Geoscience Department

New Mexico Institute of Mining and Technology

1978

Faculty Advisor: Dr. Gerardo W. Gross

TABLE OF CONTENTS

ABSTRACT

Methods to derive activation energy, relaxation times and static dielectric constant from thermally stimulated currents (TSD) have been developed. Several peak separating/cleaning techniques are described. Experimental limits and avenues of improvement have been defined. Two HP-97 calculator programs to determine 1000/T(°K), °K, °C, ΔT, ε_s and τ have been written.

The TSD technique was applied to pure ice and to ice samples doped with $NaHCO_3$ and HCl. The results for pure and $NaHCO_3$-doped ice are not conclusive since they were obtained before the TSD technique was perfected. At least four peaks were observed, the second one discharged being the principal range β. Consistent results were obtained for the HCl doped sample. Three peaks were found, the β peak at the lowest temperature. A shifting of T_m with consecutive runs at the same heating rate is apparent for all samples and may be explained by the presence of space charge, extrinsic protons or dislocations within the crystal lattice. Further avenues of research and refinement of technique are suggested.

1. INTRODUCTION

The TSD method consists of polarizing a dielectric at a fixed temperature under an electric field. By lowering the temperature the dipoles are then frozen in allignment with the electric field. The electric field is removed and the sample is warmed at a constant heating rate. As the dipoles relax becoming randomly oriented an electric current is observed. This electric current, the result of depolarization, is measured as a function of temperature.

It is hoped that the information gained by this technique will supplement as well as confirm data obtained from the more typical method of electrical bridge measurements which were made earlier on pure and doped samples of ice by this author's faculty advisor, Dr. Gerardo W. Gross, and his assistants. TSD may serve as an independent means of determining the relaxation time, τ, activation energy, A, and polarization strength, ε, of each individual spectrum.

One advantage inherent to the TSD method is the generation of a continuous set of measurements or spectrum, enabling the immediate determination of the number of spectral ranges, their relative position and strength, where it is assumed that the spectra exhibiting the largest current discharge represents the principal Debye range. This should aid the technique of straight line fitting to the spectral ranges now being utilized in electrical bridge measurements. Not now obtainable with bridge measurements, the TSD method will also serve to expand the low temperature, i.e. low frequency end of the relaxation time and

and polarization strength curves.

As of now the major difficulties in the TSD method lie in the uncertainty of peak separation and in the only fair control that is exercised over the linear heating rate. These two problems are related in as much as a slower heating rate tends to shift peaks to lower temperatures. If this be a differential effect, one peak may be shifted further than another thus aiding separation. Also since it has proved better to sandwich an ice sample between teflon foils, bridge measurements are still necessary to determine the ice to teflon thickness ratio, Q, which is used in correcting for the foils.

2. EXPERIMENTAL APPARATUS AND METHOD

The apparatus is schematically shown in Figure 1.

The sample cell design is essentially that of Gross(1977) except that a new sample holder was designed and built which makes the insertion of the ice sample easier and the electrical connections more reliable. The holder consists of a fixed top electrode and a spring-loaded bottom electrode. Attached to a thick aluminum lid, the holder is placed inside a thick walled cylindrical aluminum well which sits on an aluminum cold finger. The whole system is contained in a stainless-steel Dewar and is cooled with liquid nitrogen.

The heating mechanism consists of a heater coil (see Gross 1977) wound around the aluminum cavity which is controlled by a chromel-constantan thermocouple running from the cavity wall to a Love Model 52 proportional triac controller and Model 105 cam programmer. The cam is cut to provide linear heating and cooling rates.

A zero to 2000v d-c power supply is used to produce the polarizing field. A 100k ohm resistor installed at the front output connector serves to protect the dewar against shorts, the voltage dropping across the resistor instead of the dewar. Discharge current is measured with an ammeter built around a Keithley Model 301 operational amplifier electrometer capable of measuring currents from 10^{-14} to 10^{-7} amps.

Sample temperature is monitored by an independent copper-constantan thermocouple threaded through the holder lid and fitted into the upper electrode. Thermocouple output as well as discharge

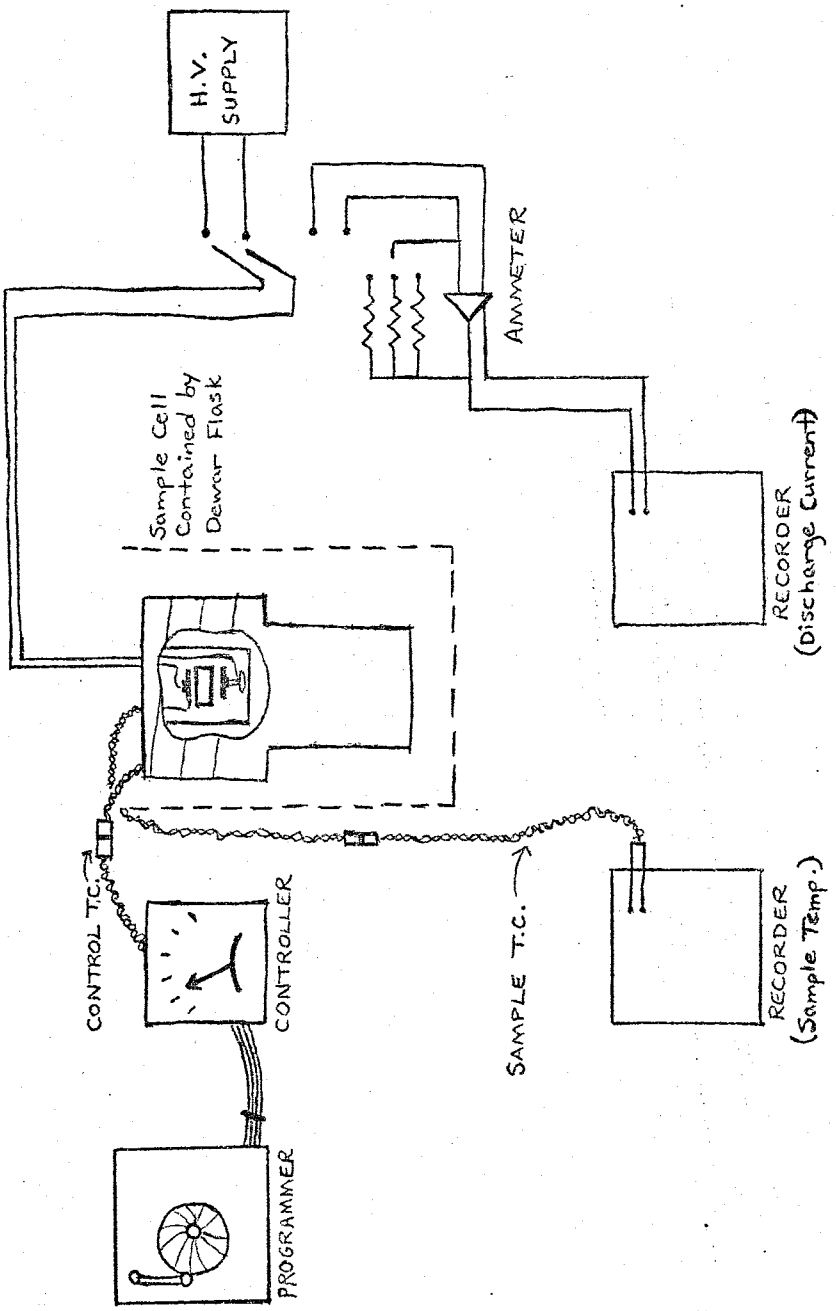

Figure 1: Diagram of experimental arrangement for TSD measurements.

current are then recorded on a two-channel Honeywell recorder (Model Electronik 195) with voltage ranges from 0.01mv to 300 volts.

Ice samples are prepared as follows: (1) An ice column is grown and sliced into disks. (2) The disk's diameter is altered to fit the sanding tools and then (3) polished to a smooth plane surface using fine grained sandpaper. To reduce the ice sample diameter, an aluminum mold was cut to the proper disk-shaped dimensions (see Figure 2 below). The mold which is at room temperature is moved towards and around the ice sample melting off its edges. Care in proceeding slowly protects the ice sample against thermal shock and shattering. A 3.5cm diameter by 0.7-1.7cm thickness are typical dimensions.

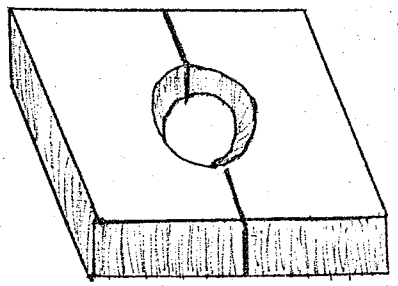

Figure 2: Mold to melt ice sample to proper diameter.

Several types of measurements are made on the ice sample--full run, determine ϵ_s run, electrical bridge measurements. The full run consists of polarizing the ice sample while its temperature is being lowered from -12°C to -194°C under a constant rate. An extraneous charge is produced often obscuring the

initial rise of the TSD curve but which can be reduced by grounding the sample cell for a period of time. This shorting time seems to depend on doping since it was found that a pure ice sample required a longer shorting period than did a HCl doped sample.

A determine ε_s measurement is made by charging at a fixed temperature, T_p. The ice sample is brought to the desired temperature and the electric field is applied for a time greater than the relaxation time, $\tau(T_p)$. The author has followed Johari(1975) in this regard by charging for a period five times that of the relaxation time expected at any particular temperature. At the completion of charging, the sample is cooled under the field to a temperature T_f such that $\tau(T_f) \gg \tau(T_p)$ to freeze in the charge. At $T=T_f$ the electric field is turned off, the cell is grounded and the temperature further lowered. The latter is necessary as a curve may discharge at a temperature lower than where it charged. Then here as in the full run, the temperature is linearly raised; the relaxation time gets shorter and as the dipoles lose their preferred orientation a discharge current is recorded.

To interpret the resultant TSD curves, electrical bridge measurements are needed. The sample cell was so designed that its output connector cables can be transferred directly to the bridge without removing the dewar cover. Measurements are made at a couple of temperatures typically around -80°C and -50°C which are fed into the computer program DIEL which outputs a semicircular Cole plot. From the right abscissa intersection,

$\varepsilon_{s\alpha}$ may be found and thus Q (from Eq.(2), Gross, 1977, p.98).

The main heater ground runs from the sample cell lid to an external switch which reads "Electrometer/Bridge". The "Electrometer" position is for the Full and Determine ε_s runs, the "Bridge" position for the electrical bridge measurements. The electrical noise generated by the pulsing of the heater is eliminated by this ground connection.

There are primarily three sources of additional noise affecting the current discharge curve. The spring-loaded screw cap which holds the wire connection to the bottom electrode may loosen after repeated thermal cycling. Sublimation of the sample occurs causing the formation of small ice crystals on the sample surface, foils and/or electrodes. These progressively cause roughness in the discharge curve as well as random spikes. If the noise gets bad, the sample may be repolished, the foils and electrodes cleaned. A sample cracking will produce a noisy signal but this can sometimes be remedied by repositioning the sample in the holder. At times the sample will even heal itself by annealing at higher temperatures during a run. Earlier it was found that the heater cable upon getting wet would produce a great deal of noise. This problem has for the time being been eliminated by drying the cable, applying RTV and wrapping it in electrical tape, but it could reoccur. There have also been intermittent failures in coaxial cables and thermocouples when connections break after frequent use.

The new sample holder was constructed and is used instead of the old sample holder of Gross(1977) for a number of reasons.

First it was found that electrical noise would be generated when the tether-like electrical connection to the top electrode was pinched by the spring through which it is threaded. It was thought this elusive source of noise was due to the formation of microcracks in the ice sample; it was only after a couple of measures were taken to repair the sample that the real cause was discovered. The two methods employed to rid the sample of the supposed microfractures were to pressurize or anneal the sample before using. A chamber was built which could supply several hundred pounds of pressure. Dry N_2 gas was used. Sample holder and chamber were both kept at -30°C for about 20 hours. Another ice sample was maintained in a silicone oil bath at -1°C for over a month. However the annealing and pressurizing of samples were abandoned when consistently smooth discharge curves were obtained after repairing the sample holder.

In addition to the above, greater ease in placing foils and sample in holder were desired and realized in the design of the new holder. Teflon rings fitted to both electrodes provide a small lip which prevents the sample from sliding out. Holes are drilled in the electrodes that thermocouples may be inserted to monitor the sample temperature. These were used at one time to measure the temperature gradient across the sample. A difference of 1°C was measured for a 6hr/full cam cycle heating rate.

Since the two holders apply different stresses to the sample, the effect of small pressures on the discharge curve could be examined. No significant difference was found in the curves for a sample run in both holders under similar conditions.

To insure that teflon did not exhibit a depolarization current, teflon foils and a teflon disk were placed in both holders and a full charging/discharging run made on them. The result was zero current discharge thus the ice sample alone is the source of the TSD response.

Instead of teflon foils, some runs were made with porous metal "disks". These consist of sintered palladium spherules and are melted onto the ice surfaces. Before placing the ice/disk system into the sample holder, it was always allowed to reach thermal equilibrium.

3. INTERPRETATION OF RESULTS

3.1 Identification of Peaks

The peaks in a multiple spectrum are tentatively labeled by their relaxation times, those with the fastest times appearing at the lowest temperatures. Spectral ranges with successively slower relaxation times will discharge at progressively higher temperatures. This means the peak associated with space charge should appear at the end of a discharging run since it has a large relaxation time.

The principal dispersion range is implicitly equated with the peak exhibiting the largest current discharge. This peak may be identified following a full run. The remaining peaks can be labeled with the assistance of existing bridge measurements made on ice samples with the same doping impurity and concentration. Knowing the relative order of relaxation times, the spectral ranges from the TSD and electrical bridge methods might be correlated. Caution should be taken in this procedure as the bridge technique may not have sensed all peaks. On the other hand, the TSD apparatus at present can only control the discharge process at a linear rate up to -50°C for a 6hr/full cycle rate. This could mean the loss of the space charge and possibly other peaks.

For every sample, a full charging run, the cooling rate linearly controlled, should be made to first determine the number and relative size (T_m) of the peaks from which the principal range is identified. This may also suggest initial polarizing temperatures, T_p, for the determine ϵ_s runs to follow.

Trial determine ϵ_s runs are then made at temperatures T_p spaced initially 5° above and below the peak temperature (T_m) of each peak and the interval is progressively narrowed on successive runs.

A tentative polarization time $t \gg \tau(T_p)$ can be deduced from the τ v.s. 1000/T curves of electrical bridge measurements if they are available for similar sample dopings. A curve is linearly extended into the desired temperature range. In addition, the curve indicates the temperature range over which the TSD system can physically respond. For relaxation times on the order of a few minutes, the dipoles relax before they can be frozen in since the large thermal mass of the TSD apparatus cannot be cooled sufficiently fast. On the other hand it may be impractical to charge for a period greater than a few days.

3.2 Activation Energy, A

The literature presents three ways to determine the activation energy: (1) initial rise method, (2) graphical integration of whole TSD curve (Bucci and Fieschi, 1966), (3) half-width temperatures of a current graph (Turnhout 1975). The initial rise method consists of measuring A from the low temperature tail of the current graph according to the equation

$$\ln i(T) = \text{const.} - A/kT \quad , \quad T < T_h \qquad (3.1)$$

where k (=1.98 cal/°K-mole) is Boltzman's constant, T(°K), the temperature, i (amps), the current and A (cal/mole), the activation energy. T_h is the temperature at which $i=\frac{1}{2}i_{max}$. A straight line results when lni is plotted as a function of 1/kT the slope of which is A. Three problems may arise which could prevent the use of the method or make the results questionable.

(1) Residual charge occurs at the start of discharge curve, (2) the peak in question discharges amid other peaks and (3) the range was not fully charged initially.

The second method is based on the relation that

$$\ln \tau(T) = \ln \tau_o + A/kT = \ln\left[\int_{t(T)}^{\infty} i(t')dt'\right] - \ln i(T) \quad (3.2)$$

or

$$\tau(T) = \left[\int_{t(T)}^{\infty} i(t')dt'\right] \Big/ \left[i(T)\right] \quad (3.2b)$$

Another straight line results from a plot of $\ln \tau$ as a function of $1/kT$ for which the slope is A. The success of this method depends on how well the different peaks can be separated.

Turnhout (1975) has devised a third method utilizing the half-width temperatures ${}_{1,2}T_h$, i.e. the temperatures at which the current discharge is half its maximum value. He derived the following equations from the implicit expression

$$j_r({}_{1,2}T_h) = \tfrac{1}{2} j_m$$

where the subscripts stand for released and maximum current density, respectively:

$$kT_m/A = 0.69117h_1 + 0.90887h_1^2 + 2.1414h_1^3 \quad (3.3)$$

$$kT_m/A = 1.0151h_2 + 0.18182h_2^2 \quad (3.4)$$

$$kT_m/A = 0.40843H + 0.24099H^2 \quad (3.5)$$

where $h_1 = 1 - {}_1T_h/T_m$, $h_2 = {}_2T_h/T_m - 1$ and $H = h_2 - h_1$. With T in °K, ${}_1T_h$ and ${}_2T_h$ represent the low and high half-width temperatures, respectively. Equations (3.3) to (3.5) are said to be accurate to within better than 0.5% for $0 \leq kT_m \leq 0.2$. The degree of certainty in the values of T_m, ${}_1T_h$ and ${}_2T_h$ depends again on how well the peaks are separated.

3.3 Relaxation time, τ

The relaxation time, τ, can either be calculated from the graphical integration method described in the previous section, or from the relation cited by Bucci and Fieschi (1966) and used by Johari (1975) in his work

$$T_m = (q\ A\ \tau(T_m)\ /\ k\ )^{\frac{1}{2}} \qquad (3.6)$$

Different heating rates, q, vary T_m thus Eq. (3.6) can be solved for τ as a function of temperature, T_m. A determine ε_s type run is used to collect such data and since the equation is independent of forming temperature, T_p, and applied voltage, V_c, values of T_p should be chosen which produce a clearly defined peak.

The author mistakenly used full runs to collect this data on pure ice samples believing this to be the method used by Johari (1975). But as he does not clearly state the type of run used in his article, the author now follows the method of Bucci and Fieschi (1966) and uses a determine ε_s type run.

A final method attributable to Dr. G.W. Gross follows. Independent of A, the relation

$$\frac{q_1}{q_n}\frac{T_{mn}^2}{T_{m1}^2} = \frac{\tau_n}{\tau_1} \qquad n = 2, 3, 4, \ldots \qquad (3.6b)$$

is derived from Eq. (3.6). A run at a heating rate of q_1 is chosen as the reference against which all other runs are compared. The values of q_1 and T_{m1} held fixed, the values of q_n and T_{mn} are determined from succeeding runs. Setting $\tau_1 = 1$ sec, Eq. (3.6b) is solved for τ_n. τ_1 and τ_n are then plotted against $1000/T_{m1}$ and $1000/T_{mn}$ respectively. A least squares line is fitted to the n points, the slope of which is A/k. Thus A(kcal/mole) is found.

3.4 Dielectric Constant, ε_s

To calculate the static dielectric constant, ε_s, a determine ε_s run is made and the discharge current as a function of temperature integrated according to the equation

$$\varepsilon_s - \varepsilon_\infty = \frac{1}{E \varepsilon_o q} \int_{T_d}^{T_u} \frac{i}{\text{Area}} \, dT \qquad (3.7)$$

where

E = applied electric field, (volts/cm)
ε_o = permittivity of free space = 8.854×10^{-14} F/cm
q = heating rate, (°K/sec)
i = current discharge, (amps)
Area = surface area of ice sample, (cm^2)
T_d = temperature at which TSD starts
T_u = temperature at which current drops to zero
ε_∞ = 3.0

which combines Equations 3.6 and 3.10 from Turnhout (1975). It should be remembered that any one ε_s value is the sum of all succeeding peaks,

$$\varepsilon_{sn} = \varepsilon_\infty + \sum_{k=1}^{n} \Delta\varepsilon_{sk}$$

which can graphically be displayed as is Fig. 3.1 below.

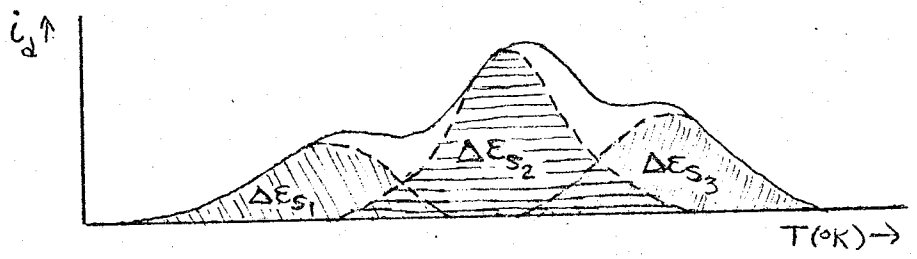

Figure 3.1: Peaks contributing to a particular value of the static dielectric constant.

3.5 Foil Corrections

Relaxation times and values of the dielectric constant must be corrected for the presence of the foils. Equations for this purpose have been worked out by Gross (1977). The value of Q, the ratio of ice to teflon thickness is determined from the right intercept called $\varepsilon_{s\alpha}$ of a Cole plot. Bridge measurements which generate the data for the Cole plot should be taken for every ice sample and repeated for a sample which has undergone extensive repolishing between runs.

Once $\varepsilon_{s\alpha}$ is known, Q is found from

$$\varepsilon_{s\alpha} = (1 + Q) \varepsilon_1$$

where $\varepsilon_1 \cong 2.1$ is the dielectric constant of the teflon foils. The dielectric constant for the principal range, ε_2, is then found from

$$\varepsilon_{s\beta} = \frac{(1 + Q) \varepsilon_1 \varepsilon_2}{Q \varepsilon_1 + \varepsilon_2}$$

The subscripts β, α etc. denote the uncorrected values of the dielectric constant computed by the method in Section 3.4 as well as the uncorrected values for the relaxation time τ found by the methods of Section 3.3.

ε_2 known, the corrected relaxation time of the principal range, τ_2, can be found from

$$\tau_\beta = \frac{Q \varepsilon_1}{Q \varepsilon_1 + \varepsilon_2} \tau_2$$

The equations above may be generalized for all high-frequency ranges according to Equations (4a) and (5a) of Gross (1977).

3.6 Separation of Peaks

From the discussion so far it should be clear how important well separated peaks are to the proper interpretation of A, τ and ε_s. Unfortunately there is at present no single method of subdividing peaks, only a combination of techniques. It is known that decreasing/increasing the heating rate shifts a peak to lower/higher temperatures. At times this could provide a partial separation. Changing the thickness of the teflon foils might also produce the desired effect (Gross, 1977).

So far the discharge curves have been such that separating the peaks simply by eye has proven effective. A slight asymmetry in the curve shape (Bucci and Fieschi, 1966) is kept in mind when constructing a single peak and of course the separate peaks must superpose to produce the original multi-spectral curve. If first order kinetics is assumed to apply, then the curve shape should be symmetrical and it would be possible to construct the whole curve from a single side portion.

Another technique to subdivide a complex curve into individual peaks is peak-cleaning. There are two variations, one worked out by Bucci and Fieschi (1966) and the other by Creswell and Perlman (1970) and Perlman (1971). The method of Bucci and Fieschi is to polarize the dielectric at T_p such that $T_{m1} < T_p < T_{m2}$ where $T_{m1,2}$ are the maxima temperatures of the superposed peaks. Then charge at T_p for an interval of time $t_p \sim \tau_1(T_p) \ll \tau_2(T_p)$. The dipoles of range 1 will be polarized at saturation while those of range 2 are for the most part randomly oriented. The TSD curve will then show only peak 1.

To obtain peak 2, both ranges are polarized to saturation and the lower temperature range is partially discharged first, the sample cooled, then discharged again to obtain the pure or nearly pure second peak.

The method of Creswell and Perlman differs slightly from the above. Assume three bands polarized at saturation. The temperature is raised to T_{PH1} to record curve (a), lowered to ambient (liquid nitrogen), raised to T_{PH2} to record curve (b), lowered again, then raised to record peak (c) as shown in Fig. 3.2. To subtract the contribution of peak (3) to curve (b) the data is first normalized to obtain curve (4) (see below). Curve (4) subtracted from curve (b) gives curve (2) and curve (2) from curve (a) gives curve (1). It is assumed T_{PH2} was high enough to remove all lower temperature peaks. The data of curve (3) are normalized to account for charge lost during the first heating. This is done as follows. To obtain curve (4), points along curve (3) up to T_{PH2} are multiplied by the correction factor 1/1-F where F is the area under (c) up to T_{PH2} divided by the total area under (c). From Fig. 3.2 the value of F is X/X+Y. Finally, a clean peak (3) is the difference between the complex curve and the sum of cleaned peaks (1) and (2).

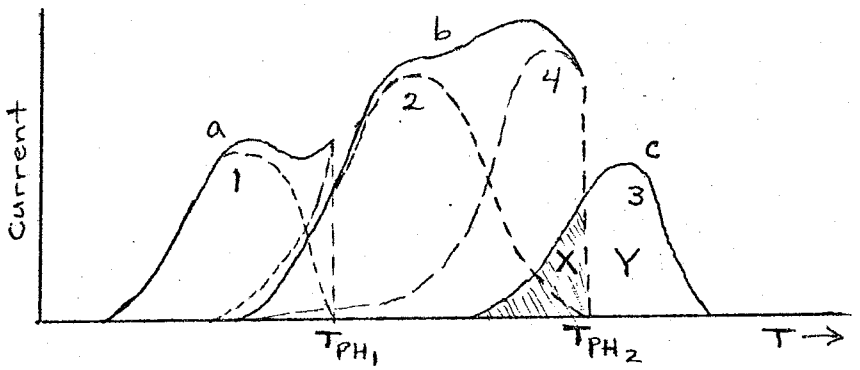

Figure 3.2: Peak-cleaning--discharge current v.s. temperature. a,b,c, are observed currents. 1,2,3 are the isolated peaks.

Application of these peak cleaning methods was difficult in practice because heating/cooling could not be stopped within one or two degrees of a desired temperature. The reasons for this deficiency were: (a) large temperature gradients between cell wall and sample holder due to the heating arrangement; (b) the large thermal inertia of the system causing thermal overshoot.

3.7 Additional Assumptions

A background current level exists on many TSD curves which does not seem to be a part of the proper discharge current. To subtract its contribution a run is continued until a static level is reached which is then taken to be the zero current level.

Discrete polarization ranges rather than a continuous distribution of polarizations is also assumed. According to Turnhout (1975) a distributed polarization exists when the τ v.s. 1000/T curve exhibits a deviation from a straight line plot for $T(°K) > T_m(°K)$. Such a deviation has been observed, but the author believes this may only be due to poor separation of peaks which introduces error in the graphical integration of τ values.

It cannot be assumed that all peaks are present and fully charged unless the total area under all peaks gives the value of $\mathcal{E}_{S\infty}$ determined from bridge measurements.

4. RESULTS

4.1 Scope of Work

Full and determine ε_s runs as well as bridge measurements were made on samples of pure ice and $NaHCO_3$ and HCl doped ice. Some runs were made with metal disks but most were made with thin teflon foils. A description of the samples used and the number and types of runs made to produce the results of this paper are contained in Table 4.1 below.

Sample #	Solute	Run #	Type Run	Disks/ Foils	Bridge Measurements
308/7 #4B	Pure	75	Full	Foils	---
		79-82	"	"	---
		85	"	"	---
		88-90	"	"	---
		101	"	"	---
308/7 #5A	Pure	109	"	Disks	---
		123	Det ε_s	"	---
308/35 #10	$NaHCO_3$	129	Full	"	---
		130	"	"	---
		132-134	"	"	---
308/35 #7	$NaHCO_3$	137-141	"	Foils	
		144	Det ε_s	"	
		146	"	"	
		148-149	"	"	$\varepsilon_{s\alpha}$=25.8
		152-153	"	"	
		155-156	"	"	
None	Pure	169-171	Full	"	---
308/35 #7	$NaHCO_3$	184-189	"	"	$\varepsilon_{s\alpha}$=25.8
302/85 E37	$4x10^{-5}$ M HCl	201	Det ε_s	"	
		203-205	"	"	
		208-210	"	"	$\varepsilon_{s\alpha}$=35.24
		214-229	"	"	
Mother solutions: $1x10^{-5}$ M $NaHCO_3$ $1x10^{-2}$ M HCl					

Table 4.1: List of runs.

4.2 Spectral Ranges

Dielectric relaxation is best described by a small number of discrete polarization ranges as opposed to a continuous

polarization distribution. The ranges correspond to the individual peaks of TSD curves. For the HCl sample studied two overlapping ranges were discovered only after a very slow heating rate was used. It may be that not all ranges for the pure, $NaHCO_3$ and HCl samples studied have been uncovered. At present the author has found 3 bands in the HCl discharge curve and at least 4 in the pure and $NaHCO_3$ discharge curves.

Unfortunately many of the TSD curves were produced from full runs rather than determine ϵ_s runs. Since the question of whether a full run can be used to supply the activation energy from initial rise and τ from graphical integration still remains, few conclusions from those runs can be made. In addition it was not until after many runs had been made that the temperature difference between cell wall and sample holder was discovered as a major source of error. This makes it difficult to ascertain the true sample temperature from the cell wall temperature which was monitored. For these reasons only a few of the full run results will be presented here, most of which have not been corrected for the temperature recording error.

The results that follow pertain to the principal range unless otherwise stated.

4.3 Pure Ice

The initial runs were done using teflon foils. Four peaks were observed; the one at the lowest temperature being the strongest is labeled the principal range, β. Since fast heating rates were used, i.e. 3 and 6 hr/full cycle, it is not known whether the main peak could have been separated into multiple

peaks. It was also observed that the fourth peak shifted toward higher temperatures after each successive run until it merged with the large current rise at the end of a run. After the sample was allowed to rest a number of days the fourth peak appeared again. The reason for this behavior is unknown however it is suggested the peak may be due to an extrinsic phenomenon. The large current discharge at the end of these runs could hide another peak. Much slower heating rates are needed to resolve this question.

The shifting also appears in the value of τ_β calculated from Eq. (3.6) with A=11.3 kcal/mole. Repeated runs made with the same heating rates of 3 and 6 hr/full cycle produced a shift in τ_β to higher temperatures. However on reversing the polarity of the electric field, τ_β appeared to shift back towards lower temperatures. This would suggest the presence of extrinsic protons which migrate out of the ice sample when subjected to an electric field over a period of time. The initial shift in τ_β is shown in Fig. 4.2(a).

The initial rise results shown in Fig. 4.1 give values of A which range from 6.75-8.5 kcal/mole. The low value as compared to 11.3 kcal/mole determined by Johari (1975) could be a result of using a full run, of peak superposition, or of the presence of impurities.

Samples were then run with porous palladium disk electrodes frozen onto the sample. The curves bear a resemblance to Johari's curves (1975) for non-aged ice samples. Instead of the current dropping nearly to zero after peaks in runs using teflon foils, the curves continue to rise after each successive

peak. This makes interpretation difficult and prompted the subsequent return to foils. Activation energies of 7.06 and 7.68 kcal/mole were derived from the slope of the lines shown in Fig. 4.2(b). They were determined from the graphical intergration of a full and determine ε_s run respectively.

The determine ε_s curve does not give true values of τ_β since the temperatures have not been corrected.

The values of $\varepsilon_{s\beta}$ derived from the runs using disks are extremely low. They range from 11 to 58 whereas values near 200 are to be expected. The discrepancy may be due to poor disk/ice contacts or to impurities.

A pure ice sample taken from a newly grown column and run with blocking electrodes finally produced a $\tau(T)$ curve which lies close to that found by Johari (1975) when the value A=11.3 kcal/mole is used with Eq. (3.6). The results are shown in Fig. 4.2(c) and the temperatures have been corrected to that of the sample holder.

The value of A=11.3 kcal/mole used in this section was derived from the initial rise method using the i/VC_g v.s. T(°K) curve at $q=2.28\times10^{-3}$ °K/sec of Fig. 2 in the Johari (1975) paper.

4.4 Pure Ice + $NaHCO_3$

All results in this and succeeding sections correspond to true sample cell temperatures.

Pure ice was doped with $NaHCO_3$ to suppress the effects of extrinsic protons suspected in causing the shifting phenomenon described in Section 4.3. The results for the principal range (β) are shown in Fig. 4.3. A number of full runs were made with

foils. Relaxation times were computed from Eq. (3.6) using A=11.4 kcal/mole (see below). The curve produced from the same sample after a slight repolishing is shifted to higher temperatures. The shift may be due to the small thickness change or perhaps to the elimination of impurities which migrated to the sample surface.

The points from another set of full runs made with disks fall along the line produced from the runs made with foils. This indicates the ice/disk system acted like an ice/foil system. Since the latter must still be corrected for the presence of the teflon foils this might explain the poor ε_2 values gotten earlier with disks.

The τ_β curve produced from a determine ε_S run and from which the value A=11.4 kcal/mole was found is shown plotted in Fig. 4.3 (Run 153). The calculated value of ε_2 is 99 which again differs from an expected value of around 200. Errors in the integrated area of the discharge curve, the estimated area of the sample surface, and the averaged value of the heating rate may be responsible. The data of this ε_S run (β_α range and β range) coincide with the above mentioned full runs made with foils after repolishing the sample. On the contrary, one might have expected a closer correspondence with the data before repolishing (Runs 137-141, etc.). An overestimate in the area of a peak will always shift a τ v.s. 1000/T curve upwards. Since the author's first approximation for the high temperature portion of the β peak was overestimated and because a well superposed β' peak on the low temperature side of the β peak could be present,

the upward shift of the determine ε_s line away from the first data set is understandable.

Fig. 4.3 shows the results for two other spectral ranges tentatively labeled β_α and β'. Both curves (determined from full runs) exhibit the shift due to sample repolishing. In this case the $\tau_{\beta\alpha}$ line produced from the determine ε_s curve falls correctly amidst the first data set. The slope gave A as 7.6 kcal/mole. Because no isolated β' peak appeared an A value of 9.3 kcal/mole taken from bridge measurements was used to calculate $\tau_{\beta'}$ with Eq. (3.6). Activation energies of 5.62 and 6.66 kcal/mole were derived from the initial rise method on full runs using disks. Results are plotted in Fig.4.4.

As another reference the Worz and Cole (1969) line for pure ice is plotted in Fig. 4.3.

4.5 HCl - 4.12×10^{-5} M (Foils)

Three spectral ranges appeared after slow heating rates were introduced. The peaks are labeled β, β_α and α and discharge from low to high temperatures respectively. Results are shown in Figs. 4.5-4.8.

Fig. 4.5 shows the initial rise plots which give values for A which vary from 6.25-7.37 kcal/mole. Both the 12 and 20 hr/full cycle heating rates give the more reliable value of 6.25 kcal/mole from a least squares fit of the curves.

The method of Eq. (3.6b) gave an activation energy of 5.6 kcal/mole after the points were fitted with a least squares line. The average of this and the preceeding two values of 6.25 kcal/mole gave the value A=6.03 kcal/mole which is used in all succeeding calculations.

Values of τ computed graphically from Eq. (3.2) are plotted on Fig. 4.6 for different heating rates. The τ_β line from electrical bridge measurements is plotted as a reference. The bend in the 6 hr/cycle curves is a result of adding to the area of the β peak that of the initially hidden intermediate peak, β_α. The bending is not as apparent on the other curves where the influence of β_α has been accounted for. τ curves for the slow heating rates mutually agree and give the activation energy as 6.03 kcal/mole. They lie close to the τ_β curve extrapolated from bridge measurements having an activation energy of 6.1 kcal/mole.

Relaxation times computed from Eq. (3.6) are plotted in Fig. 4.7 for A=6.03 kcal/mole. The points fit the curves of Fig. 4.6 except for the two gotten from faster heating rates which lie at the highest temperatures. T_m of the β peak was shifted due to the presence of the β_α peak.

Fig. 4.8 gives the values of ε_2. The problem of detection at fast relaxation times makes suspect those values of ε_2 at the higher temperatures.

The study is not yet complete, a few more points will be taken at lower temperatures to extend the τ_β and ε_2 curves. Results on the β_α and α curves are yet to be compiled.

4.6 Methods of determining τ

The graphical method of determining τ generates much more of a τ v.s. 1000/T curve than does Eq. (3.6). It also reveals whether one has fully isolated a peak as a poor separation will subsequently appear as a hump or bend in the plotted curve.

However this is not responsible for the sharp rise at the low temperature end of the curve. The bend there is a consequence of describing the initial rise as an exponential function. This means that in the graphical integration method, τ tends to infinity as i_d goes to zero.

Since a curve rather than a single point is produced from the graphical method, the superposition of curves from different runs on the same graph will indicate something of the reproducibility of results.

4.7 Reproducibility of $T_{m\beta}$

Successive runs made with the same heating rate (6 hr/cycle) and field polarity on a sample of $NaHCO_3$ doped and on a sample of HCl doped ice reveal a shifting trend in $T_{m\beta}$ toward higher temperatures.

Determine ε_s runs 144, 146, 148, 149 and 152 shows $T_{m\beta}$ for a $NaHCO_3$ doped sample shifting from 155.2°K to 173.4°K. Although the T's have not in this case been corrected to the true sample temperature, all of these runs were begun at nearly the same temperature ($\sim 2°$ variance) and so corrections should not eliminate the shift occurring in $T_{m\beta}$ with time.

The 4×10^{-5} M HCl doped sample in runs 205, 208-210 showed a shift in $T_{m\beta}$ from 100.26°K to 104.9°K. After the sample sat for 12 hours or so without charging, the next run (214) gave $T_{m\beta}$=100.6°K. The sample sat again for 30 hours before run 215 gave $T_{m\beta}$=101.75°K. Runs 216-219 were then made on successive days and showed a shift in $T_{m\beta}$ from 103.4°K to 107.0°K.

5. AVENUES OF FURTHER INVESTIGATION

5.1 Experimental Apparatus

Modification of the temperature control system is still needed. At present a change of 10% or more in the linearity of heating rates faster than 6 hr/full cam cycle is not unusual, yet much of the TSD interpretation is based upon this premise. Finer control of the temperature is needed to make peak-cleaning a reliable method of peak separation. To obtain values of $\tau(T_m)$ according to Eq. (3.6) at higher temperatures heating rates faster than 6 hr/full cycle are a necessity. Work to improve the situation has begun. Small heaters placed inside an aluminum cylinder which fits snugly around the new sample holder will be used to better control the heating rate. The cylindrical insert also reduced the air space through which heat convection currents had to pass. Noise problems due to these heaters have yet to be solved.

It would also be desirable to devise a method which would freeze in polarization charge at temperatures corresponding to fast relaxation times. Presently the system cannot be cooled to a temperature T where $\tau(T) \gg \tau(T_p)$ before the dipoles have relaxed.

The differential heater of Gross (1977) or its equivalent should be reintroduced to minimize the vertical temperature gradient across the ice. This was measured only once with the new sample holder at a heating rate of 6 hr/full cam cycle.

Thermocouples fail to register the true sample temperature

because of their length and since they pass through a large temperature gradient from inside to outside the dewar. Since determine ε_s runs require a strict control of the temperature within the sample cell, both control and sample thermocouples should be compensated for fluctuations in room temperature.

Because of the heating arrangement and large thermal mass of the system, it has proved difficult to set the sample temperature at desired values of T_p for the determine ε_s runs. At present one first makes gross adjustments on the cam which controls the temperature of the cell wall. After waiting an hour or more for cell wall and sample holder to reach thermal equilibrium, the sample temperature monitored with a separate thermocouple is then read off the chart recorder scale. If this millivolt reading is not that of the desired value T_p the cam is readjusted and the process above is repeated however many times it takes to set the sample temperature at T_p. It is suggested therefore that a separate controller be installed which is easily set to fractional values of T_p and then maintains that temperature setting within the sample holder.

Special copper backed teflon foils have been purchased in an attempt to reduce the air gap between electrodes and sample. It is not known yet what if any effect this will cause.

It was hoped this author would write a computer program to analyze the data. However experimental setbacks and interpretative difficulties prevented this. The major problem in writing a program lies in isolating peaks in a way that data can be easily digitized. To at least simplify the process of

digitizing the total current discharge and temperature as a function of time a printer is being built to monitor these quantities. Programs have been written and recorded for use on a HP-97 calculator to do the following: (1) Convert microvolts to degrees Celsius and Kelvin and (2) to calculate 1000/T(°K) and (3) the temperature interval, ΔT. A separate program calculates the values of (4) τ and (5) ε_s.

5.2 Experimental Results

The shifting of the maxima temperature, T_m, with time for pure and doped ice samples needs further investigation as it may show whether extrinsic protons cause different positions and slopes (activation energies) of the τ v.s. 1000/T curves found by various investigators, such as Auty and Cole (1952), Worz and Cole (1969), and Johari (1975). The study of HCl doped samples should be continued and expanded to those doping impurities which have been studied using electrical bridge measurements.

Improved methods of peak separation are desired, and the effect of increasing teflon thickness to this end are yet to be looked into. In addition the question of insufficient peak separation v.s. continuous distribution of relaxation times still remains.

There is also the question as to whether the change of slope of the τ v.s. 1000/T curve for pure ice could be due to dislocations assuming the sample to be free of impurities. Annealing of pure ice samples should be tried in an attempt to eliminate these dislocations and thus possibly extend the

linear portion of Auty-Cole curve to lower temperatures.

The problem of why ε_2 values were so much lower than those found by other investigators needs to be studied.

The question of whether full runs may be used in conjunction with Eq. (3.6) still remains but might be answered with a closer look at the time-temperature superposition theory of Gross (1968) referred to by Johari (1975).

6. CONCLUSIONS

The TSD method appears to be a viable method to supplement and substantiate results obtained from electrical bridge measurements. It is an independent means of determining activation energy, relaxation time and dielectric constant or alternatively the polarization strength once Q is found by the electrical bridge method. TSD extends τ and ϵ curves to the low temperature range.

The variable results found for pure and $NaHCO_3$ doped ice are thought to be due to trace impurities and poor electrical contact between disks and ice. However because full rather than determine ε_s runs were used and cell wall rather than sample temperature were monitored only guarded conclusions can be drawn.

The problem of peak separation was solved in the HCl study by decreasing the heating rate.

The relaxation time curves for the HCl sample are in good agreement with a curve obtained from bridge measurements.

Consistent values of the activation energy and relaxation times were obtained when slower heating rates were used.

In spite of the scatter, a trend in the ε_2 data can be discerned.

7. LIST OF REFERENCES

Auty, R.P., and R.H. Cole (1952): Dielectric properties of ice and solid D_2O. J. Chem. Phys. 20: 1309-1314.

Bucci, C., R. Fieschi, and G. Guidi (1966): Ionic thermocurrents in dielectrics. Phys. Rev. 148: 816-823.

Creswell, R.A., and M.M. Perlman (1970): Thermal currents from corona charged mylar. J. Appl. Phys. 41: 2365-2375.

Gross, B. (1968): Time-temperature superposition theory for electrets. J. Electrochem. Soc. 115: 376-381.

Gross, G.W. (1977): Dielectric dispersion and conductivity of ammonium compounds in ice. Research proposal submitted to the National Science Foundation. (143 pp.).

Johari, G.P., and S. J. Jones (1975): Study of the low-temperature "transition" in ice I_h by thermally stimulated depolarization measurements. J. Chem. Phys. 62: 4213-4223.

National Bureau of Standards (1974): Thermocouple Reference Tables Based on the IPTS-68. NBS Monograph 125, p. 401 (quartic equation for -200 to 0°C).

Perlman, M.M. (1971): Thermal currents and the internal polarization in carnauba wax electrets. J. Appl. Phys. 42: 2645-2652.

van Turnhout, J. (1975): Thermally Stimulated Discharge of Polymer Electrets. Elsevier, Amsterdam. (335 pp.).

Worz, O., and R.H. Cole (1969): Dielectric properties of ice I*. J. Chem. Phys. 51: 1546-1551.

8. CAPTIONS FOR FIGURES

Figure 4.1: Initial rise curves for pure ice principal range. Thin foils, 6 hr/full cycle.

Figure 4.2: Principal relaxation times for pure ice.

(a) Shift of τ_β (calculated from Eq. 3.6) with successive runs.

● 3 hr/cycle (runs 75, 79-82)

人 6 hr/cycle (runs 85, 88-90)

(b) τ_β determined from graphical integration of TSD curve (Eq. 3.2b).

⊙ full run, foils (#101)

△ full run, disks (#109)

× determine ε_s run, disks (#123)

(c) ⊡ $\tau_\beta(T_m(q))$, foils, A=11.3 kcal/mole; from bottom to top, runs:

169 (5 hr/cy);
170 (7 hr/cy);
171 (9 hr/cy).

Figure 4.3: Relaxation times for ice containing 1×10^{-5} M $NaHCO_3$. Ranges β_α, β, and β'.

Full runs made with teflon foils.

○ β_α range (runs 137-141)

□ β range (runs 137-141, det ε_s runs 153,155,156)

△ β' range (runs 137-141)

● β_α range (runs 184-189)

■ β range (runs 184-189)

▲ β' range (runs 184-187, 189)

} After repolishing

Full runs made with sintered palladium disks

× β range (runs 129,130,132-134).

Determine ε_s run with teflon foils (before repolishing)

▽ β_α range

▼ β range

Figure 4.4: Initial rise curves for pure ice + $NaHCO_3$ for β' range. Disks.

Figure 4.5: Initial rise curves for 4.12×10^{-5} M HCl + Foils, principal range.

Figure 4.6 a & b: Principal relaxation times for 4.12×10^{-5} M HCl + Foils.

Figure 4.7: Principal relaxation times for 4.12×10^{-5} M HCl + Foils. Determined from Eq. (3.6).

Figure 4.8: Principal dielectric constant for 4.12×10^{-5} M HCl + Foils.

Figure 4.1

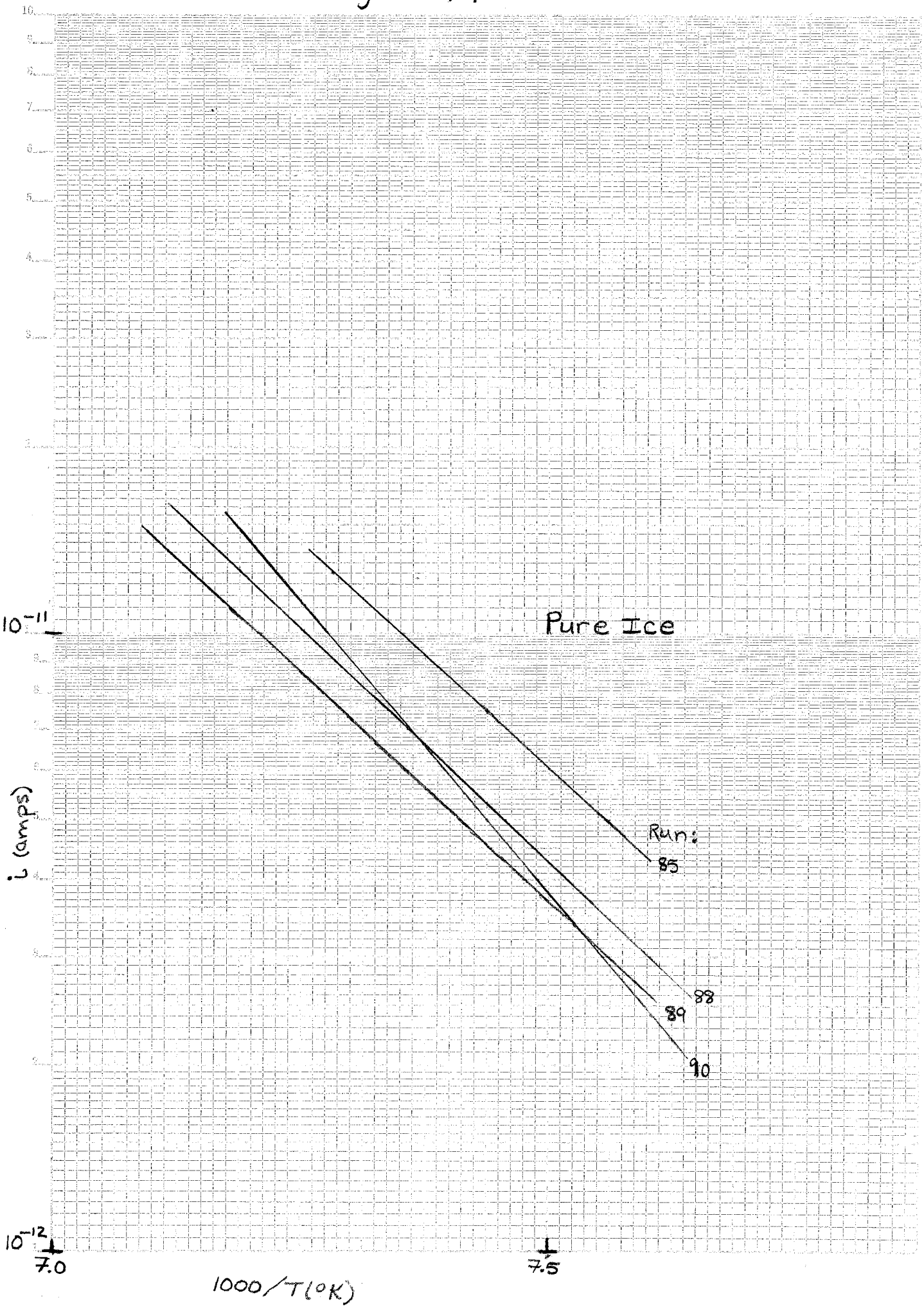

Figure 4.2

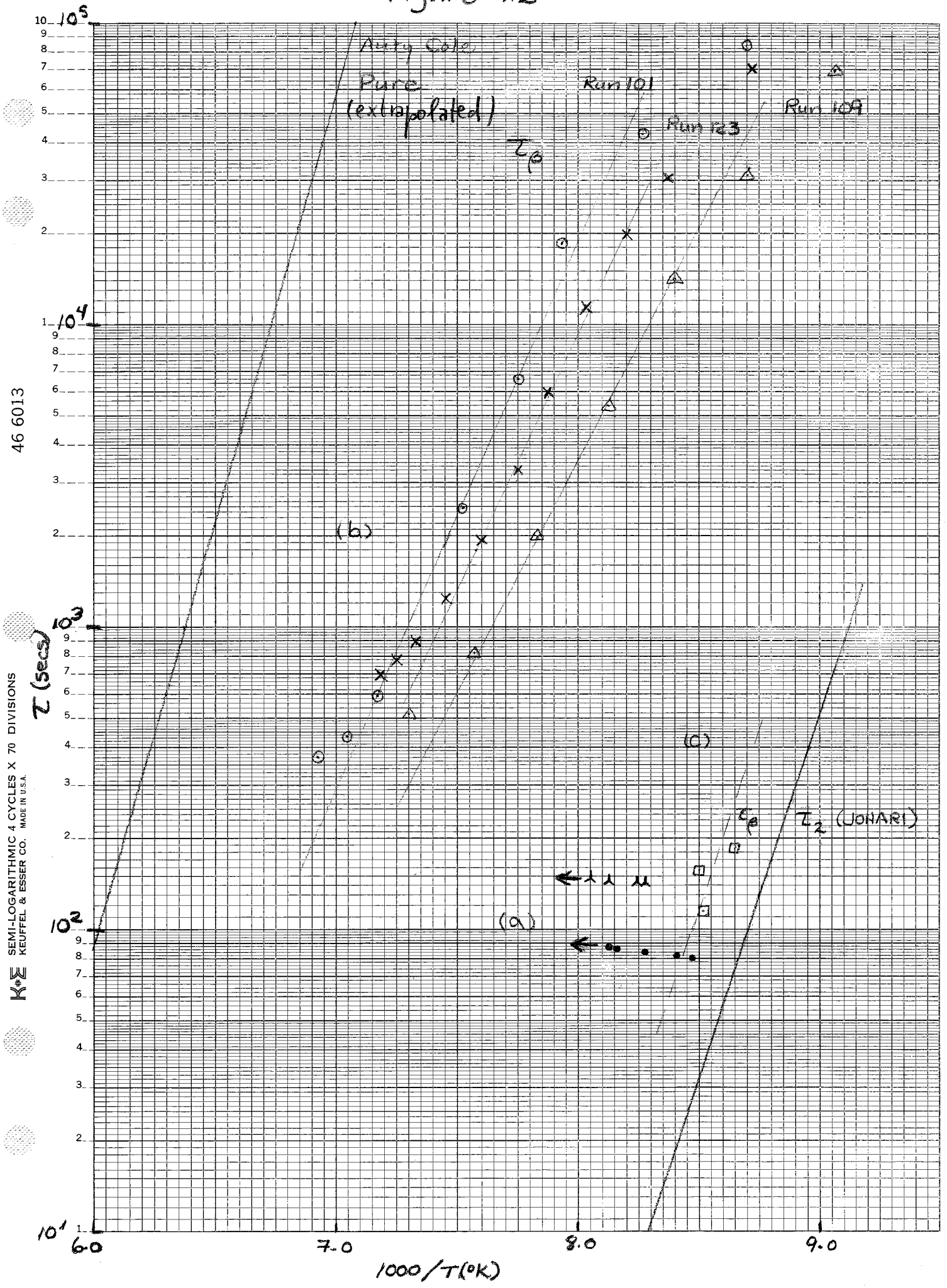
Ruby Coil
Pure
(extrapolated)
Run 101
Run 123
Run 104
τ_p
(b)
(c)
(a)
τ_e
τ_2 (JOHARI)
τ (secs)
10^5
10^4
10^3
10^2
10^1
6.0
7.0
8.0
9.0
1000/T(°K)
46 6013
SEMI-LOGARITHMIC 4 CYCLES X 70 DIVISIONS
KEUFFEL & ESSER CO. MADE IN U.S.A.

Figure 4.3

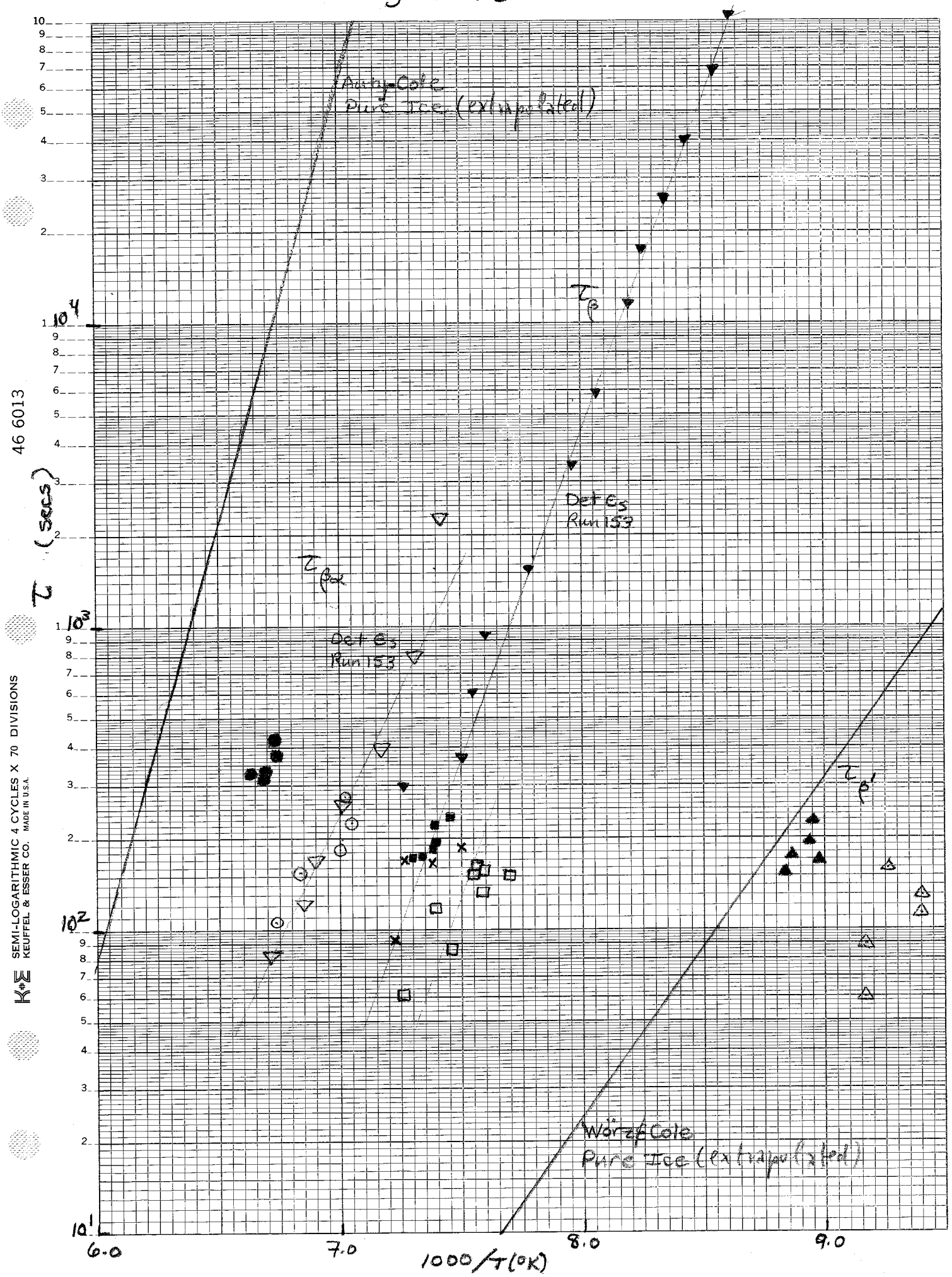
Auty-Cole
Pure Ice (extrapolated)
τ_D
Det e_5
Run 153
τ_{Det}
Det e_5
Run 153
$\tau_{D'}$
Wörz-Cole
Pure Ice (extrapolated)
τ (secs)
10^4
10^3
10^2
10^1
6.0
7.0
8.0
9.0
1000/T(°K)
46 6013
SEMI-LOGARITHMIC 4 CYCLES X 70 DIVISIONS
KEUFFEL & ESSER CO. MADE IN U.S.A.

Figure 4.4

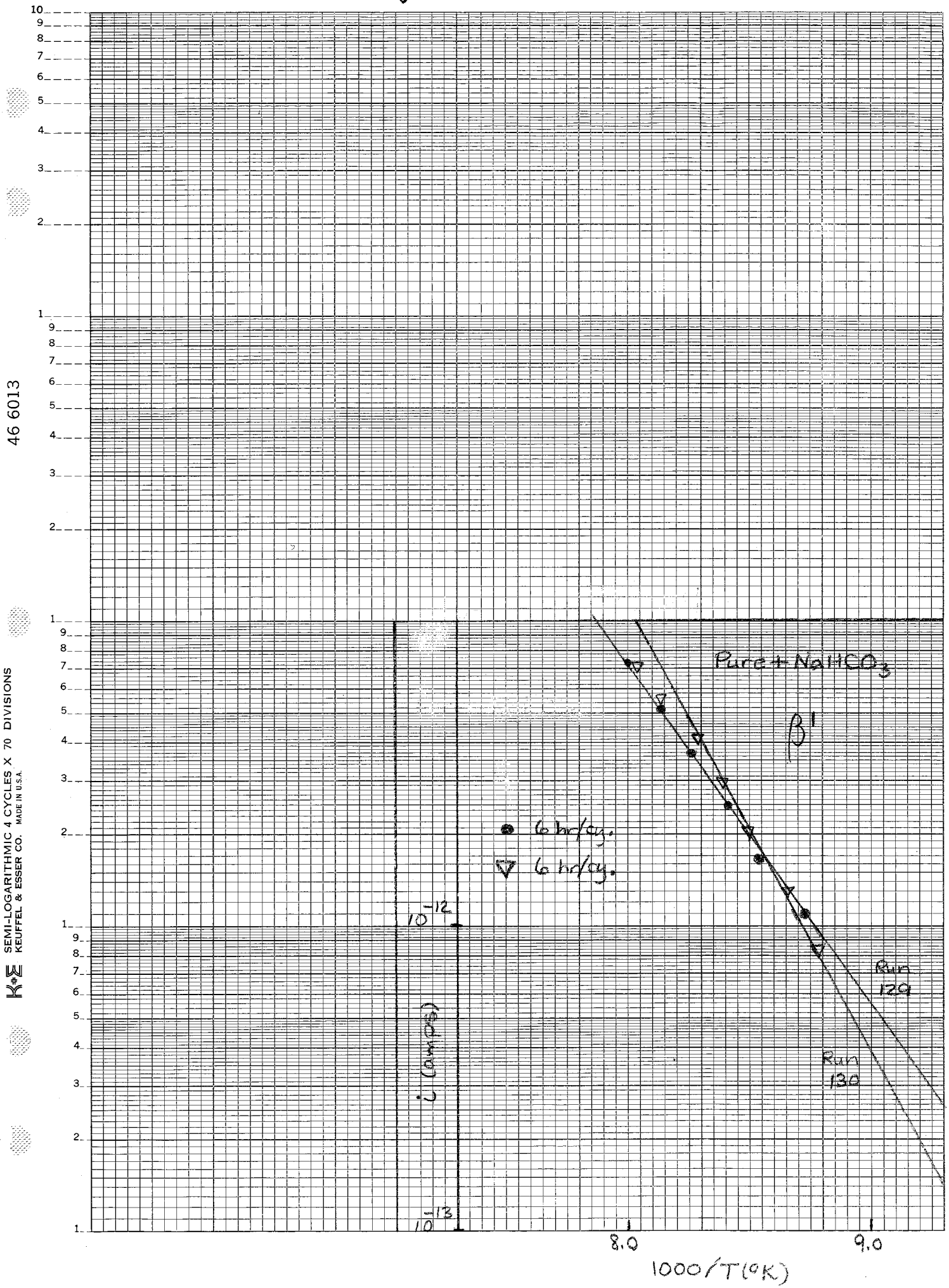
Pure + NaHCO3
β'
● 6 hr/cy.
▽ 6 hr/cy.
Run 129
Run 130
10^-12
10^-13
J (amps/cm²)
8.0
9.0
1000/T(°K)
46 6013
SEMI-LOGARITHMIC 4 CYCLES X 70 DIVISIONS
KEUFFEL & ESSER CO. MADE IN U.S.A.

Figure 4.5

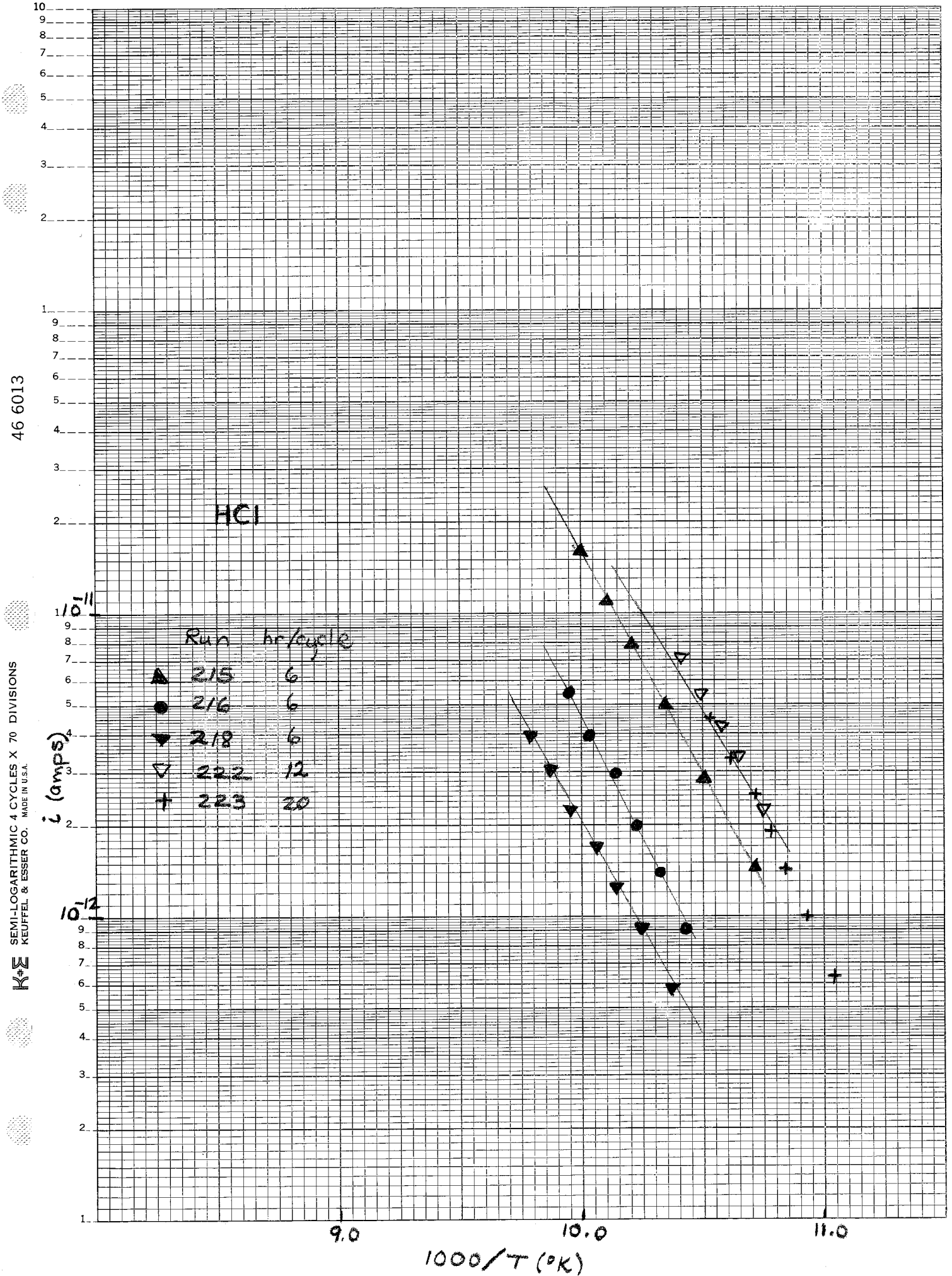
HCl
Run hr/cycle
215 6
216 6
218 6
222 12
223 20
i (amps)
10^-11
10^-12
9.0
10.0
11.0
1000/T (°K)
46 6013
SEMI-LOGARITHMIC 4 CYCLES X 70 DIVISIONS
KEUFFEL & ESSER CO. MADE IN U.S.A.

Figure 4.6a

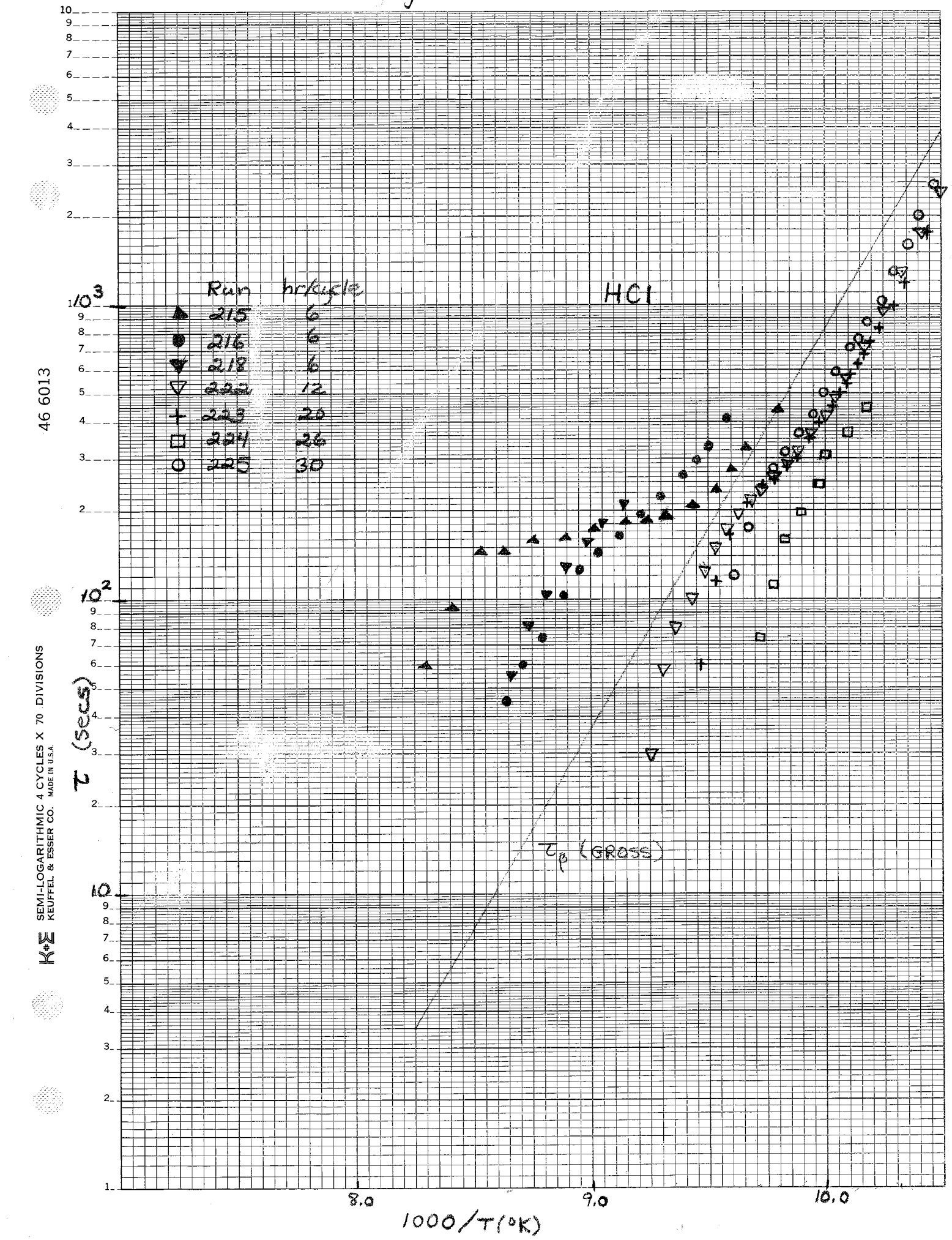
Run
hr/cycle
215
6
216
6
218
6
222
12
223
20
224
26
225
30
HCl
τ (secs)
τ_p (GROSS)
1000/T(°K)
8.0
9.0
10.0
10^3
10^2
10
1
46 6013
KE SEMI-LOGARITHMIC 4 CYCLES X 70 DIVISIONS
KEUFFEL & ESSER CO. MADE IN U.S.A.

Figure 4.6b

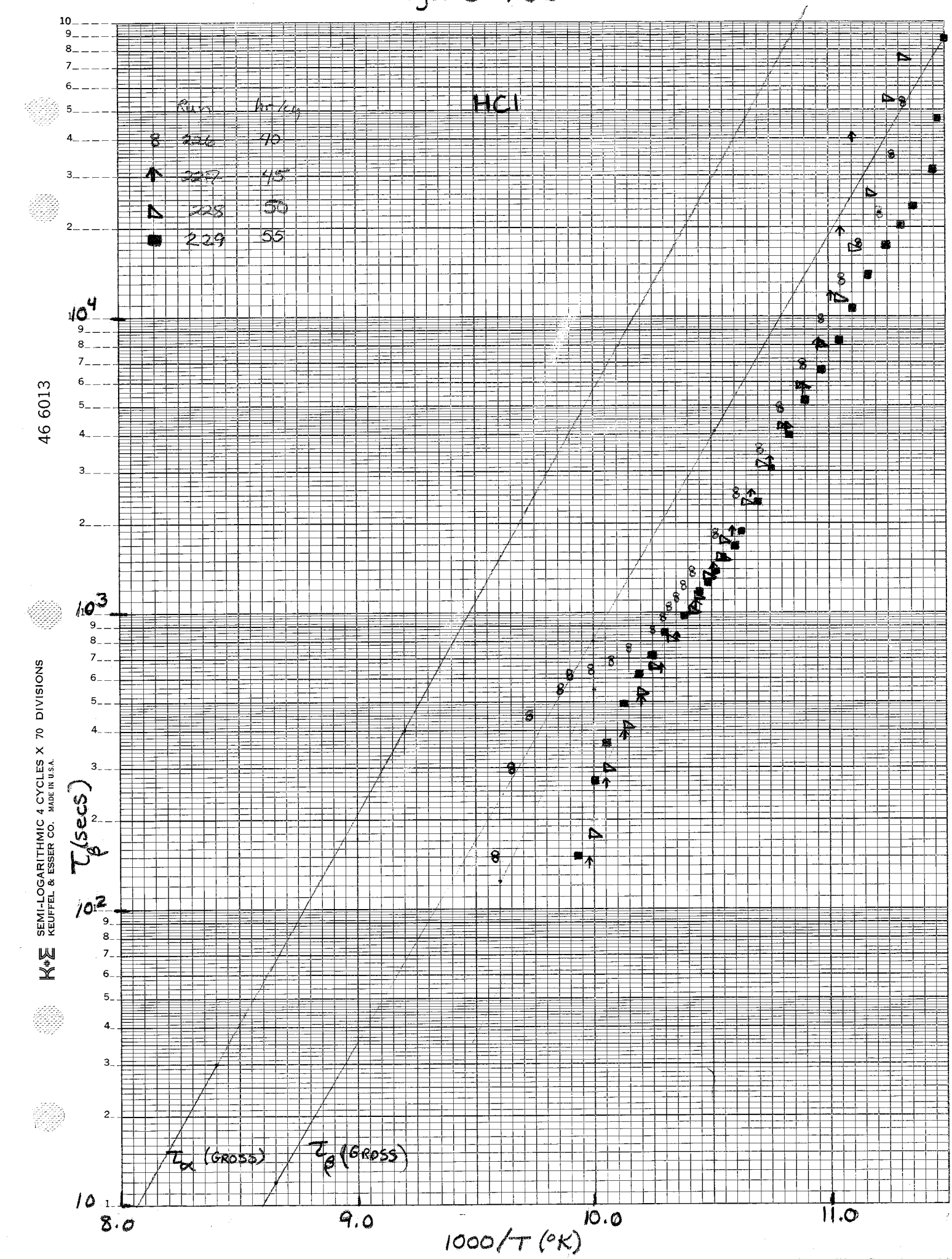
HCl
Run
hr/kg
328 40
327 45
328 50
329 55
10^4
10^3
10^2
10
T_β (secs)
T_α (GROSS)
T_β (GROSS)
8.0
9.0
10.0
11.0
1000/T (°K)
46 6013
SEMI-LOGARITHMIC 4 CYCLES X 70 DIVISIONS
KEUFFEL & ESSER CO. MADE IN U.S.A.

Figure 4.7

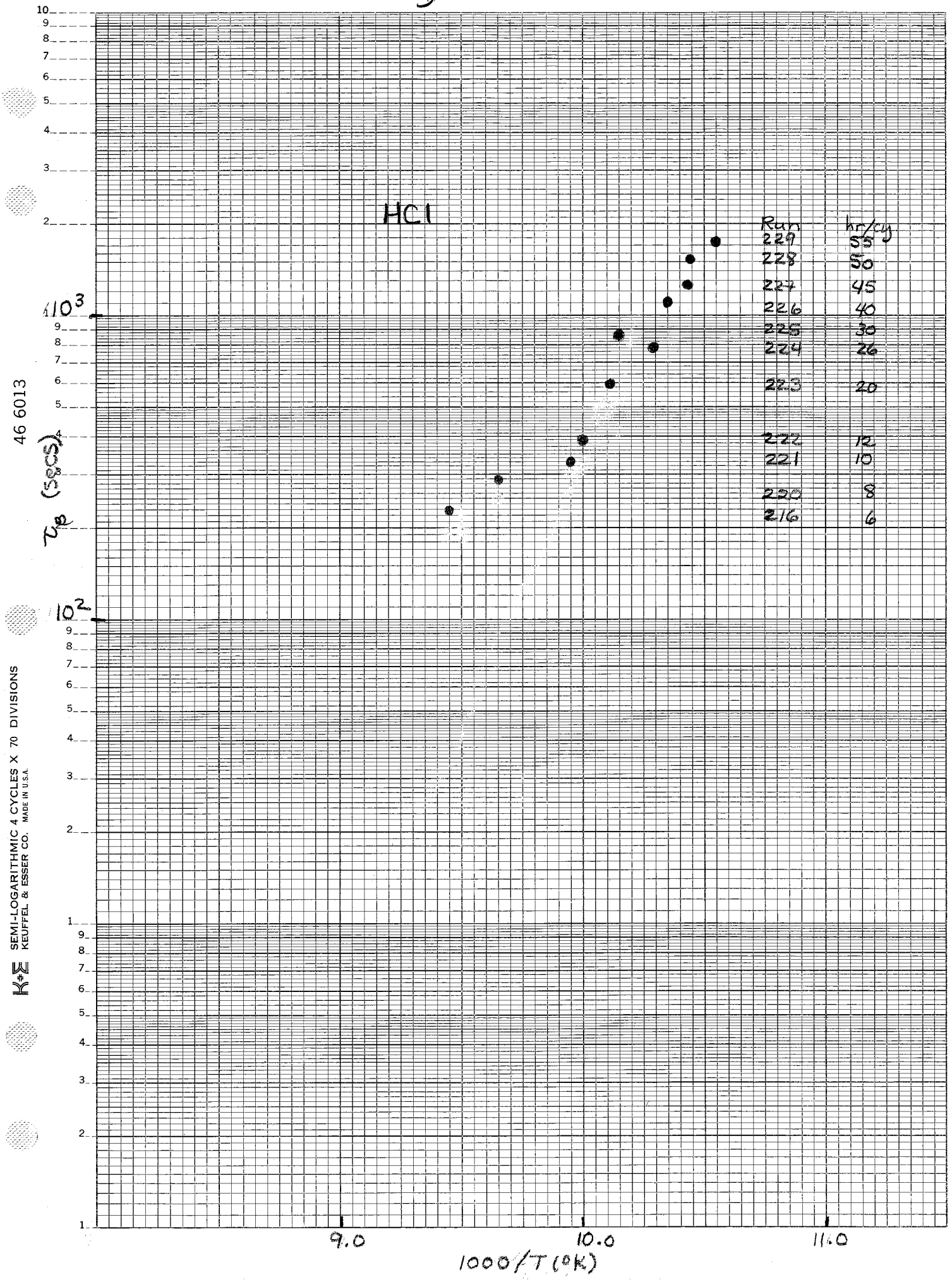
HCl
Run
229
228
227
226
225
224
223
222
221
220
216
hr/cy
55
50
45
40
30
26
20
12
10
8
6
τ_B (secs)
10^3
10^2
9.0
10.0
11.0
1000/T (°K)
46 6013
KE SEMI-LOGARITHMIC 4 CYCLES X 70 DIVISIONS
KEUFFEL & ESSER CO. MADE IN U.S.A.

Figure 4.8

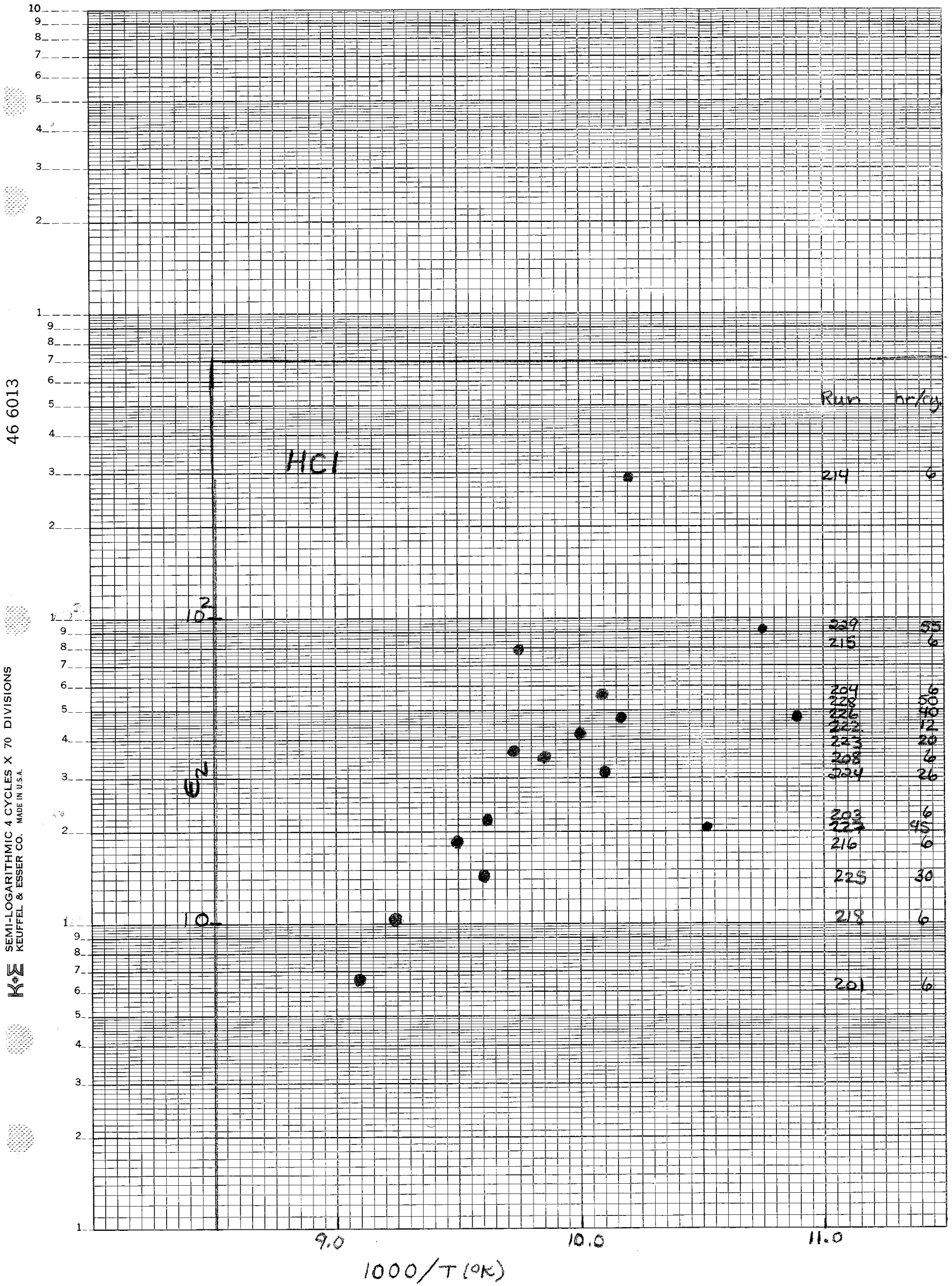
HCl
Run hr/cy
214 6
229 35
215 6
209 6
228 50
226 40
223 12
223 20
208 6
224 26
203 6
224 45
216 6
225 30
218 6
201 6
10^2
10^1
9.0
10.0
11.0
1000/T (°K)
46 6013
SEMI-LOGARITHMIC 4 CYCLES X 70 DIVISIONS
KEUFFEL & ESSER CO. MADE IN U.S.A.

9. APPENDIX

9.1 Digitizing data by hand

To digitize TSD curves by hand a zero current level on the record trace is first chosen. Separation of peaks is next done by eye and penciled in with due attention paid to curve shape (slightly asymmetric with a sharper current drop on high temperature side) and to the fact that the isolated peaks must add to reproduce the original complex curve. The curves are extrapolated at both ends to reach the zero current level.

A resultant curve is divided into straight line segments denoting intervals of time, Δt, and temperature, ΔT. The area under each section is to be integrated and summed successively from the high to low temperature end of the curve. This is done by HP-97 calculator and the program listed in Appendix 9.3. To integrate the areas the rule of trapezoids is used, namely

$$\text{trapezoidal area} = \tfrac{1}{2}(i_{D_j} + i_{D_{j+1}})\,\Delta t \ , \quad j=0,1,2,\ldots$$

where Δt is either a time or temperature interval (Δt=secs and ΔT=^{o}K) depending on whether τ or ε_s is being calculated.

The length of each line segment is chosen to follow closely that of the TSD curve, therefore the length varies over different portions of a curve. When the initial rise method is to be used the low temperature end is more finely divided. The number of divisions made was also dictated by the density of points desired for a τ v.s. 1000/T plot and to keep the time

required for such multiple calculations at a reasonable level. Segments of equal length were chosen only when it appeared they fit a curve well.

The discharge current, i_d, and its corresponding temperature are noted at each division. The two pens recording i_d and T are offset by $1\frac{1}{2}$ small divisions on the recording chart and must be corrected for when reading off T values. The temperature is normally recorded on the more sensitive channel of the chart recorder with the zero set off scale to accomodate a 1mv full span. The mv readings are entered as negative μv values into the calculator program listed in Appendix 9.2 which computes $1000/T(^\circ K)$, $^\circ K$, $^\circ C$ and ΔT for each data point. ΔT for each line segment is then used in the graphical integration of ε_s done within the program of Appendix 9.3. Since the chart speed is known, Δt(secs) is found directly from the chart record and is also entered as data into the program of Appendix 9.3 to determine τ from graphical integration.

The programs are written such that after they compute each $1000/T(^\circ K)$, $^\circ K$, $^\circ C$, ΔT, ε_s and τ value they stop to allow one to print the results. From this printed data, the final value of ε_s namely $\Delta\varepsilon_s$ which is the total area under any particular peak is found. It corresponds to the integral in Eq. (3.7). Substitution of $\Delta\varepsilon_s$ into Eq. (3.7) gives ε_s which is then corrected for the presence of the teflon foils.

9.2 Temperature program

Enter program from magnetic card. To use do following:

Instructions	Press	Display
	0, f a	0.00 00
Data input	$-\mu v(j)$	
	R/S	$1000/T_j(°K)$
Print 1000/T	R/S	$°K_j$
Print °K	R/S	$°C_j$
Print °C	R/S	$\|\Delta T\| = \|°C_j - °C_{j-1}\|$
Print ΔT	R/S	$°C_j$
	(go to data input)	

The equation used to determine °C from microvolts (μv) was taken from NBS Monograph 125 (1974, see Ref.). A listing of the program follows:

```
001  *LBL A   21 16 11
002   CLRG      16-53
003   STO2      35 02
004  *LBL 1     21 01
005    R/S        51
006   ENT↑       -21
007   STO0      35 00
008     2          02
009     .         -62
010     3          03
011     0          00
012     3          03
013     7          07
014     0          00
015     9          09
016    EEX         -23
017    CHS         -22
018     2          02
019     X          -35
020   STO1      35 01
021   RCL0      36 00
022    X↑          53
023     2          02
024     .         -62
025     9          09
026     0          00
027     7          07
028     8          08
029     0          00
030     3          03
031     9          09
032    EEX         -23
033    CHS         -22
034     E          06
035     X          -35
036   ST-1  35-45 01
037   RCL0      36 00
038     3          03
039    Y^          31
040     7          07
041     .         -62
042     1          01
043     9          09
044     4          04
045     5          05
046     8          08
047     1          01
048     0          00
049    EEX         -23
050    CHS         -22
051     1          01
052     0          00
053     X          -35
054   ST-1  35-45 01
055   RCL0      36 00
056     4          04
057    Y^          31
058     1          01
059     .         -62
060     0          00
061     0          00
062     4          04
063     1          01
064     5          05
065     4          04
066     3          03
067    EEX         -23
068    CHS         -22
069     1          01
070     3          03
071     X          -35
072   ST-1  35-45 01
073     2          02
074     7          07
075     3          03
076   RCL1      36 01
077     +          -55
078   STO2      35 02
079     1          01
080     0          00
081     9          09
082     0          00
083   RCL2      36 02
084     ÷          -24
085    R/S         51
086   RCL2      36 02
087    R/S         51
088   RCL1      36 01
089    R/S         51
090   RCL3      36 03
091     -          -45
092    CHS         -22
093    R/S         51
094   RCL1      36 01
095   STO3      35 03
096   GTO1      22 01
097    RTN         24
098    R/S         51
```

9.3 Integration program (ε_s and τ)

Enter program from magnetic card. To use do following:

Instructions	Press	Display
	0, f b	0.00 00
Enter $i_{d_{j+1}}$	$i_{d_{j+1}}$	
	R/S	$i_{d_{j+1}}$
Enter i_{d_j}	i_{d_j}	i_{d_j}
	R/S	$(i_{d_{j+1}} + i_{d_j})^{\frac{1}{2}}$
Enter ΔT	ΔT	$\Delta T = T_{j+1} - T_j$
	R/S	$\sum_{j=0}^{n} \frac{1}{2}[i_{d_{j+1}} + i_{d_j}]\Delta T$
Print ε_s	R/S	$(i_{d_{j+1}} + i_{d_j})^{\frac{1}{2}}$
$\Delta t = t_{j+1} - t_j$	Δt	t
	R/S	τ_{j+1}
Print τ_{j+1}	R/S	

(go to data input)

The program successively adds the areas under each line segment from high to low temperature end. ε_s is only an intermediate sum, with the final value being $\Delta\varepsilon_s$ the total area under a peak. The values of τ_{j+1} to be plotted versus $1000/T_{j+1}$ are generated in the program according to Eq. (3.2b). A listing of the program follows:

```
001  *LBL0  21 15 12
002   CLRG     16-55
003   STO0     35 00
004  *LBL1     21 01
005    R/S        51
006   ENT↑       -21
007   STO1     35 01
008    R/S        51
009      +       -55
010      2          02
011      ÷       -24
012   STO2     35 02
013    R/S        51
014      ×       -35
015   ST+3  35-55 03
016   RCL3     36 03
017    R/S        51
018   RCL2     36 02
019    R/S        51
020      ×       -35
021   ST+0  35-55 00
022   RCL0     36 00
023   RCL1     36 01
024      ÷       -24
025    R/S        51
026   GTO1     22 01
027    RTN        24
028    R/S        51
```